

7-6-1987

Characteristics of an Electric/Magnetic Quadrupole Detector for Low Voltage Scanning Electron Microscopy

M. Brunner

Research Laboratories of Siemens AG

R. Schmid

Research Laboratories of Siemens AG

Follow this and additional works at: <https://digitalcommons.usu.edu/microscopy>



Part of the [Biology Commons](#)

Recommended Citation

Brunner, M. and Schmid, R. (1987) "Characteristics of an Electric/Magnetic Quadrupole Detector for Low Voltage Scanning Electron Microscopy," *Scanning Microscopy*: Vol. 1 : No. 4 , Article 3.

Available at: <https://digitalcommons.usu.edu/microscopy/vol1/iss4/3>

This Article is brought to you for free and open access by the Western Dairy Center at DigitalCommons@USU. It has been accepted for inclusion in Scanning Microscopy by an authorized administrator of DigitalCommons@USU. For more information, please contact digitalcommons@usu.edu.



CHARACTERISTICS OF AN ELECTRIC/MAGNETIC QUADRUPOLE DETECTOR
FOR LOW VOLTAGE SCANNING ELECTRON MICROSCOPY

M. Brunner* and R. Schmid

Research Laboratories of Siemens AG, ZT ZFE FKE 24, Otto-Hahn-Ring 6,
D-8000 Munich 83, FRG

(Received for publication March 06, 1987, and in revised form July 06, 1987)

Abstract

The electric/magnetic quadrupole detector allows efficient detection of secondary electrons in low voltage scanning electron microscopy without introducing disturbing aberrations. The original detector of this type was built in 1986; it has now been equipped with scintillator-photomultiplier assemblies on both positive electrodes. Their signals, A and B, can be combined to A+B or A-B, thus enhancing or suppressing different types of contrast. The aberration disc produced by the present design of detector was estimated to have a diameter of 10 nm. Experimentally, no deterioration of image resolution was observed. The collection efficiency was predicted to be 26 % and can be better than 65 % with an optimized collector size. For experimental determination, the detector was first calibrated by reflecting the primary beam of known current towards the scintillators. The detected proportion of secondary electrons was subsequently determined from the detected signal. The efficiency was found to be 20 % which is in agreement with the theoretical value.

Introduction

Scanning electron microscopes (SEMs) are commonly equipped with a detector located to one side of the sample to collect secondary electrons. The positive extraction field of the detector does not noticeably disturb the focused spot of the primary beam as long as the SEM is operated at high primary energies (e. g., 10 keV to 30 keV). However, SEMs are progressively being used at low voltages (e. g., 0.5 keV to 2 keV) to serve as inspection and metrology tools in integrated circuit fabrication. Electron beam testing, which also involves low energies, uses different types of energy-selective detector below or above the lens, all laterally extracting secondary electrons. The extraction results in a deflection of the primary beam and an enlargement of the spot size (Pawley, 1984). Symmetrical arrangements of two detectors (Volbert and Reimer, 1980) avoid beam deflection but cause aberrations.

A new type of detector proposed by Zach and Rose (1986) and built and tested by Schmid and Brunner (1986) overcomes these problems. This detector uses the well-known effect of a Wien filter to differentially affect electrons travelling in opposite directions. The electric and magnetic fields are tuned to cancel out their effect on the primary beam. Secondary electrons travelling in the opposite direction, however, are efficiently deflected towards the collector electrodes. Calculations by Zach and Rose (1986) show inadmissible aberrations for the conventional Wien filter but predict promising characteristics for the electric/magnetic quadrupole arrangement. The quadrupole detector was therefore built and tested as previously reported (Schmid and Brunner, 1986). The first version of the detector, however, only used one of the positive electrodes to generate a detector signal. The detector has now been improved to take advantage of both positive electrodes for signal formation. This doubles the detection efficiency and also allows different combinations of both signals to be displayed.

Key Words: Scanning electron microscopy, low voltage, detector, quadrupole, contrast, critical dimensions, metrology, inspection.

*Address for correspondence:

M. Brunner
Research Laboratories of Siemens AG
Otto-Hahn-Ring 6, D-8000 München 83
West-Germany; Phone No. : (49) 89/636-44175

Design and Operating Considerations

Fig. 1 shows the design of the electric/magnetic quadrupole detector. It differs from an earlier arrangement (Schmid and Brunner, 1986) in that both positive detector electrodes and their scintillators are attached into two separate multipliers. The detector is mounted directly below the final lens in the present arrangement but can, in principle, be used above the lens as well. The distance between opposite electrodes is 15 mm and the overall height of the detector is 10 mm. This allows relatively short working distances along with good collection efficiency even with large samples below a flat lens.

The aberrations introduced by the electric-/magnetic quadrupole detector affecting the low energy primary beam were calculated by Zach and Rose (1986). From their formulas, the radius of the aberration disk caused by the current detector design can be estimated to be less than 10 nm if operating with ± 200 V on the electrodes and a 1 keV primary beam having 2 eV energy spread and $2 \cdot 10^{-2}$ rad aperture. In practice it has been found that the detector has no noticeable influence on the resolution of the SEM even when operating below 1 kV. The same operating conditions theoretically allow 26 % of the emitted secondary electrons to be detected (Zach, private communications). A larger positive electrode extending from the pole piece to the sample would allow more than 65 % collection efficiency (Zach and Rose, 1986).

Measurement of Detector Efficiency

For comparing different detectors it is desirable to know the proportion of all emitted secondary electrons which are collected and converted into a signal. Theoretically this proportion should be more than 26 % with the present detector arrangement (Zach and Rose, 1986). The proportion actually detected was determined in the following way:

1) In the first step the detector signal resulting from a known input current of electrons on the scintillator was calibrated (Fig. 2 a). For this purpose the primary beam of 500 eV energy was reflected from the sample holder towards the scintillators by applying -1 kV externally to the holder (Brunner, 1983) and positioning the beam successively at both detectors in the image shown in Fig. 3, which is compressed in one direction and stretched in the other by the effect of the quadrupole fields on the beam as it passes from the sample holder upwards to the detector. The current of the primary beam was determined beforehand by using a Faraday cage. An input current on the scintillators of $I_P^+ = -2 \cdot 10^{-12}$ A resulted in $U_{DA}(I_P^+) = 2.1$ V on one and $U_{DB}(I_P^+) = 1.75$ V on the other amplifier. The detector adjustments including photomultiplier and amplifier settings were kept unchanged during the following sequence.

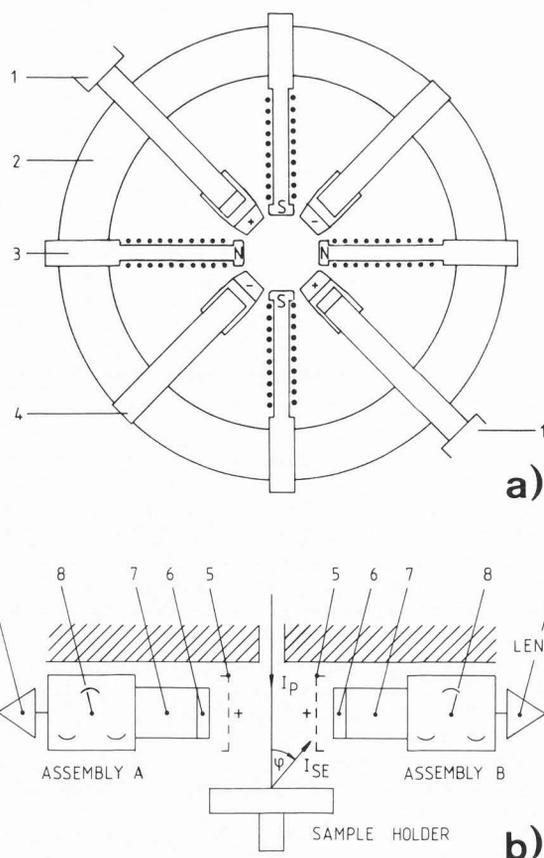


Fig. 1. Electric/magnetic quadrupole detector, a) top view; 1 = scintillator-photomultiplier assembly A and B, 2 = ferromagnetic ring, 3 = pole piece, 4 = negative electrode; b) side view, 5 = positive electrode, 6 = scintillator, 7 = light pipe, 8 = photomultiplier, 9 = pre-amplifier, I_P = primary current, I_{SE} = current of secondary electrons.

2) In the next step, the total current of true secondary electrons I_{SE} ($E_{SE} < 22$ eV) emitted upon impact of the primary beam on a platinum aperture was determined (Fig. 2 b and c). The specimen current to ground I_G resulting from a primary current $I_P = -5.85 \cdot 10^{-12}$ A was measured to be $I_G = 5.8 \cdot 10^{-12}$ A. This current equals the sum of the rest of all the currents on the sample (Fig. 2 b):

$$I_G = I_P - I_{SE} - I_{BE} = 5.85 \cdot 10^{-12} \text{ A.} \quad (1)$$

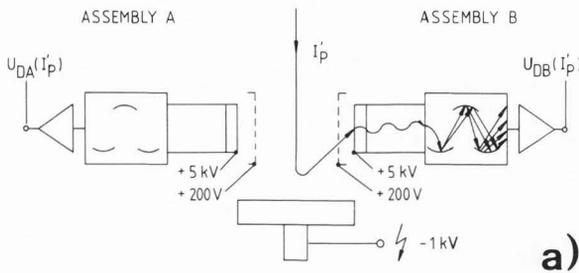
The current $I_P - I_{BE}$ was determined by measuring the specimen current I_G^+ with +22 V applied to the sample and no positive extraction fields (Fig. 2 c):

$$I_G^+ = I_P - I_{BE} = -4.8 \cdot 10^{-12} \text{ A.} \quad (2)$$

The emitted current of true secondary electrons I_{SE} was thus:

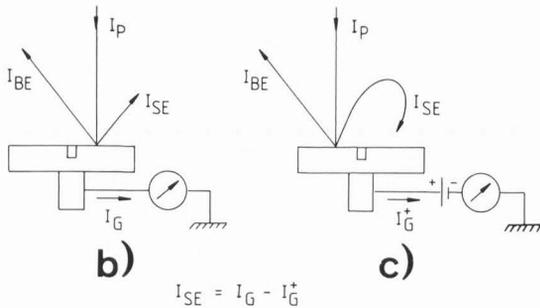
$$I_{SE} = I_G - I_G^+ \approx 10^{-11} \text{ A.} \quad (3)$$

STEP 1



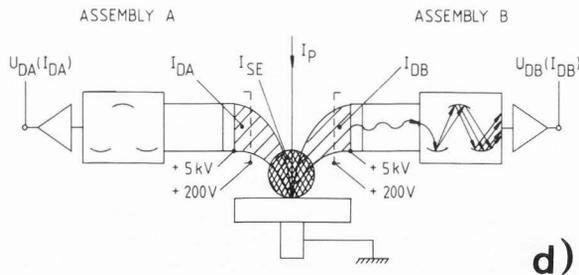
I_p' = primary current during calibration
 $U_{DA}(I_p')$ = output signal of assembly A, I_p' on scintillator
 $U_{DB}(I_p')$ = output signal of assembly B, I_p' on scintillator

STEP 2



I_p = primary current
 I_{SE} = current of true secondary electrons
 I_{BE} = current of backscattered electrons
 I_G = current to ground

STEP 3



I_p = primary current
 I_{SE} = current of true secondary electrons
 I_{DA} = current of proportion detected by ass. A
 I_{DB} = current of proportion detected by ass. B
 $U_{DA}(I_{DA})$ = output signal of assembly A, I_{DA} on scintillator
 $U_{DB}(I_{DB})$ = output signal of assembly B, I_{DB} on scintillator

3) In the last step, the detected portion of all emitted true secondary electrons was determined. The total secondary-electron current of $I_{SE} = 10^{-11}$ A caused signals of $U_{DA}(I_{DA}) = 1$ V and $U_{DB}(I_{DB}) = 0.9$ V. The proportions of the total current detected by each scintillator result from the calibration in step 1:

$$I_{DA} = \frac{I_p'}{U_{DA}(I_p')} U_{DA}(I_{DA}) = 10^{-12} \text{ A} \quad (4)$$

and

$$I_{DB} = \frac{I_p'}{U_{DB}(I_p')} U_{DB}(I_{DB}) = 10^{-12} \text{ A} \quad (5)$$

Each scintillator thus detects $I_{DA}/I_{SE} = I_{DB}/I_{SE} = 10\%$ of the total emitted current of true secondary electrons, thus yielding 20% detector efficiency. The difference from the theoretical value of 26% is within the limits of measurement accuracy and the accuracy of calculations.

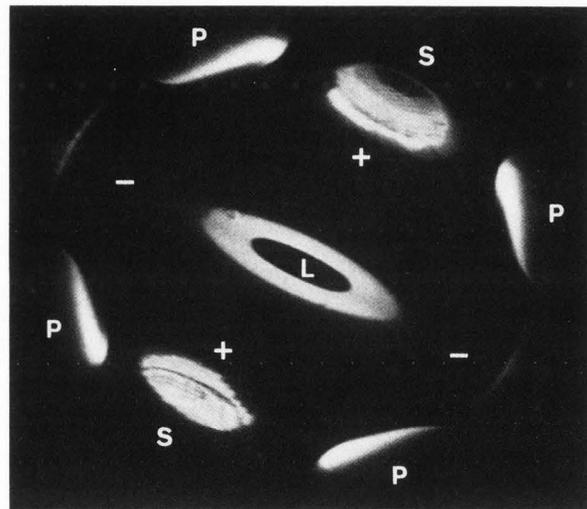


Fig. 3. Image obtained by scanning the beam of Fig. 2 a. The scintillators S appear bright, the pole pieces of the detector P and the bottom of the lens L can also be seen.

← Fig. 2. Measurement of detector efficiency $(I_{DA} + I_{DB})/I_{SE}$. a) signal calibration; b) determination of $I_p - I_{BE} - I_{SE}$; c) determination of $I_p - I_{BE}$, I_{SE} is suppressed by positive bias, d) determination of I_{DA} and I_{DB} from U_{DA} and U_{DB} respectively.

Combinations of Detector Signals

Volbert and Reimer (1980) demonstrated the display of different sample contrasts by different signal combinations from two opposite detectors (Rose, 1977). In low voltage applications, however, the strong field caused by this arrangement disturbs the primary beam. In contrast, the quadrupole detector tested here allows the signals of its two photomultipliers to be combined, thus yielding similar results with low energy primary beams.

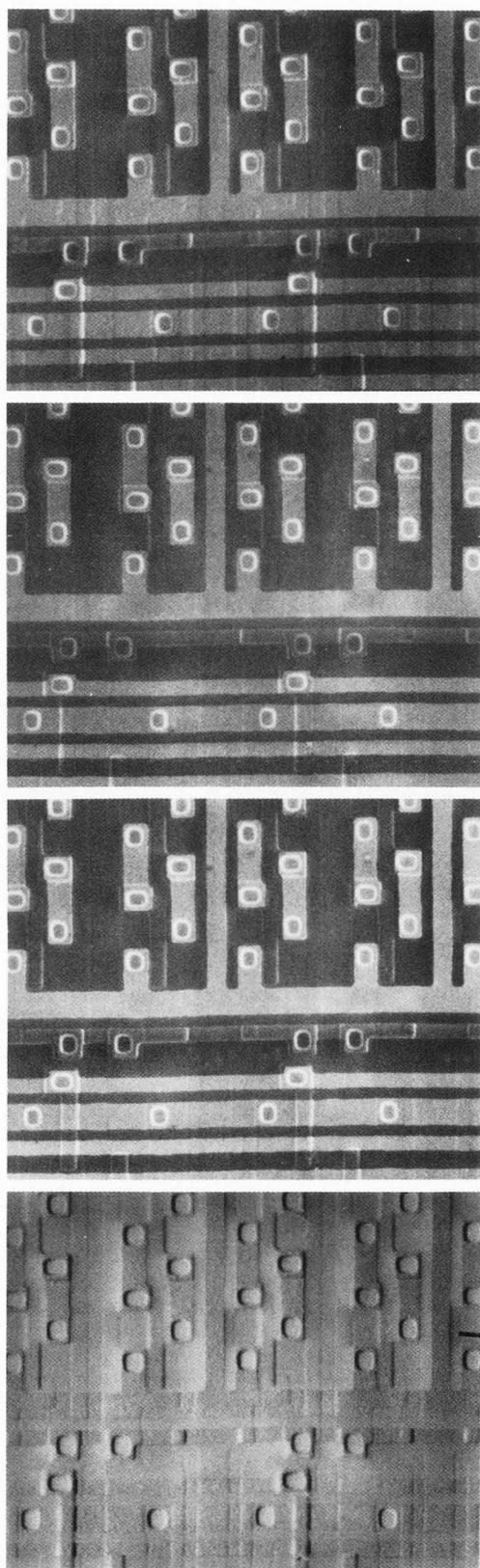
The detector separates emitted secondary electrons depending on their initial momentum. Electrons leaving the sample within the angular range of $\phi = 0$ to $\phi = -90^\circ$ with respect to normal exit are attracted to the left collector A while the trajectories of those electrons emitted in the range of $\phi = 0$ to $\phi = +90^\circ$ end up on the opposite side B. Microstructure edges oriented towards detector A therefore appear bright in the corresponding image (Fig. 4 a) while edges oriented in the opposite direction appear dark. Detector B correspondingly interchanges bright and dark edges (Fig. 4 b).

This shadow contrast is suppressed in the signal combination A+B (Fig. 4 c), thus highlighting different materials and the structure edges independently of their orientation towards the detector. The edge contrast is due to the enhanced emission on the sloped side walls of the lines. The material contrast causes metal lines on the surface of the integrated circuit to appear bright while lines buried under the top layer only show up by their bright edges. This signal is useful for quantitative measurements of critical dimensions because it is independent of the detector position (Jensen and Swyt, 1980, Postek and Joy 1986a,b, Brunner and Schmid, 1987).

Material and edge contrasts are suppressed by displaying the signal A-B (Fig. 4 d) while enhancing the shadow contrast. This highlights the sample topography and is useful for inspecting integrated circuits. It allows prominent and recessed structures to be distinguished by the shadows at their edges.

Conclusions

The electric/magnetic quadrupole detector for low voltage SEM application is now used with scintillator-photomultiplier assemblies on both positive electrodes. The two signals of output A and B may be combined to A+B enhancing material and edge contrasts or A-B enhancing shadow contrast. The A+B signal is especially suitable



a)

b)

c)

d)

100 μm 

Fig. 4. SEM images of an integrated circuit, primary energy 900 eV. a) signal A, b) signal B, c) A+B signal highlighting material and edge contrasts, d) A-B signal highlighting shadow contrast.

for quantitative measurements of critical dimensions on integrated circuits while the A-B signal facilitates inspection. Although the theoretically possible collection efficiency of an optimized design has not yet been attained, detection on large wafers or masks below a flat final lens has improved. The collection efficiency may be increased by enlarging the collector size. Location of the detector above the final lens may be advantageous but has not yet been investigated.

References

Brunner M. (1983). Simulation of backscattered electrons by reflection of primary electrons applied to optimization of detector designs. *Appl. Phys. Letters* 43, 391 - 393.

Brunner M, Schmid R. (1987). Electron-Beam Metrology and Inspection. *Microelectronic Engineering* 1987, in press.

Jensen S, Swyt D. (1980). Sub-micrometer length metrology: problems, techniques and solutions. *Scanning Electron Microsc.* 1980; I: 393 -406

Pawley J. (1984). Low voltage scanning electron microscopy. *J. of Microscopy* 136, 45-68.

Postek MT, Joy DC. (1986a). Microelectronics dimensional metrology in the scanning electron microscope. Part I. *Solid State Technology* 11, 124-150.

Postek MT, Joy DC. (1986b). Microelectronics dimensional metrology in the scanning electron microscope. Part II. *Solid State Technology* 12, 77-85.

Rose H. (1977). Nonstandard imaging methods in electron microscopy. *Ultramicroscopy* 2, 251-268.

Schmid R, Brunner M. (1986). Design and Application of a Quadrupole Detector for Low-Voltage Scanning Electron Microscopy. *Scanning* 8, 294 -299.

Volbert B, Reimer L. (1980). Advantages of two opposite Everhart-Thornley detectors in SEM. *Scanning Electron Microscopy* 1980; IV: 1 - 10.

Zach J, Rose H. (1986). Efficient Detection of Secondary Electrons in Low-Voltage Scanning Electron Microscopy. *Scanning* 8, 285 - 293.

Discussion with Reviewers

K.-R. Peters: Figure 3 demonstrates that a strong signal is produced by PE inside the detectors between positive electrodes and scintillators. This signal component may also be produced by BSE. What effect does this component have on your SE collection efficiency measurement? Do you have means to qualify this background component?

Authors: You are right, the backscattered electrons contribute to the signal and simulate a higher detector efficiency. This can be corrected in the measurement by reading the detector signal U_{DB} (backscattered) and U_{DA} (backscattered) in step 2 when a positive bias is applied to the sample. The corrected collection

efficiency results by using $U_{DA} (I_{DA}) - U_{DA}$ (Backscattered) and $U_{DB} (I_{DB}) - U_{DB}$ (Backscattered) in eq. 4 and 5. In our measurement, however, the contribution of the backscattered electrons was relatively small and the absolute accuracy of the measurement is assumed to be in the order of 3 % anyway. Although several parts of the detector appear bright in Fig. 3 the total acceptance angle of these parts converting backscattered electrons to secondary electrons is only in the order of 7%. The yield of secondary electrons δ on the platinum sample, which was used for these measurements, is close to $\delta=1$ while the yield of backscattered electrons is about $n=0.4$. 3 % of the 20 % efficiency which was measured may therefore originate from backscattered electrons.

Z. Radzimski: The collection efficiency depends strongly on the energy spectrum of secondary electrons. What values were chosen for the calculations which yield 65 % and 26 % collection?

Authors: A typical energy spectrum of secondary electrons was used (see Zach and Rose, 1986).

Z. Radzimski: In your development of a quadrupole detector you have gone from one detector to a two detector system. What about a higher order of electric magnetic multipoles system in which four detectors would be used. Such a system is a proven configuration for good topography imaging and reconstruction.

Authors: Our suggestion is to use the quadrupole arrangement with four scintillators, two of which represent the positive electrodes and the other two representing the negative electrodes. The function of the two pairs of scintillators can be interchanged by switching the voltages and currents. The signals of only two opposite detectors contribute to the image in each setting. Higher order multipoles further reduce aberrations but, on the other hand, also reduce collection efficiency (Zach and Rose, 1986).

K.-R. Peters: How do you explain shadow contrasts in terms of e-beam/specimen interactions?

Authors: This question probably arises because the term shadow contrast was used instead of topography contrast. This was done because edge contrast is caused by surface topography but is suppressed by recording A-B. Shadow contrast originates from secondary electrons being screened by adjacent surface structures. It also arises from differently tilted areas which preferably emit secondary electrons towards one of the two scintillators. Detailed discussion was published by Volbert and Reimer (1980).

K.-R. Peters: Are shadow contrasts selectively imaged on planes of normal orientation to the scintillators?

Authors: Yes

K.-R. Peters: Are shadow contrasts observed independently from the material composition of the specimen?

Authors: Yes, almost.

K.-R. Peters: At what magnifications and voltages does the detector produce recognizable aberrations?

Authors: This was not investigated experimentally but was considered theoretically by Zach and Rose (1986).

J.B. Pawley: Could you please add some dimensions to Figure 1 and also indicate the number of ampere turns needed to satisfy the Wien condition at 1 and 5 kV with ± 200 V on the electrodes?

Authors: The relevant mechanical dimensions are given in the text. At 1 kV approximately 10 ampere turns are needed to satisfy the Wien condition at ± 200 V on the electrodes (4 ampere turns at 5 kV).

J.B. Pawley: Is it necessary to have both: positive and negative electrostatic voltages, or would + and 0 be sufficient? Do the voltages change with the beam voltage?

Authors: The electrodes should be biased symmetrically to achieve ground potential on the optical axis. Either the currents or the voltages have to be changed with the beam voltage.

J.B. Pawley: What additional complications or advantages might result from mounting the detector above the lens?

Authors: The working distance can be minimized but the contrast effects will probably be changed by the influence of the magnetic lens-field on the trajectories of the secondary electrons.